Supporting Information

Reconfigurable Liquid Crystal Elastomer Director patterns for Multi-Mode Shape Morphing

Xianbing Zeng[1], Tianfeng Zhou[1,2,], Lei Li[1], Juncai Song[1], Ruijue Duan[1], Xiang Xiao[1], Baiqian Xu[1], Guanghao Wu[1], Yubing Guo[1,*]*

[1] School of Medical Technology, Beijing Institute of Technology, 100081 Beijing, China

[2] School of Mechanical Engineering, Beijing Institute of Technology, 100081 Beijing, China

Corresponding Author: * zhoutf@bit.edu.cn, yguo@bit.edu.cn

1. Materials

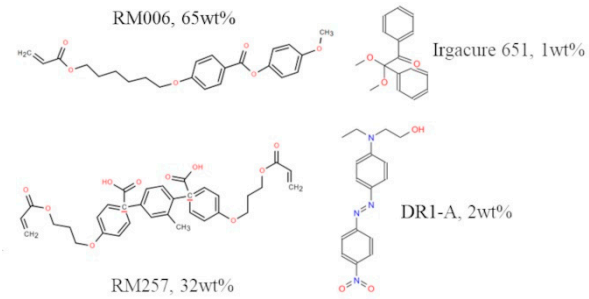

Figure S1. Chemical composition of LCEs and the corresponding weight ratios.

2. Effect of different UV glues on LCE shape morphing

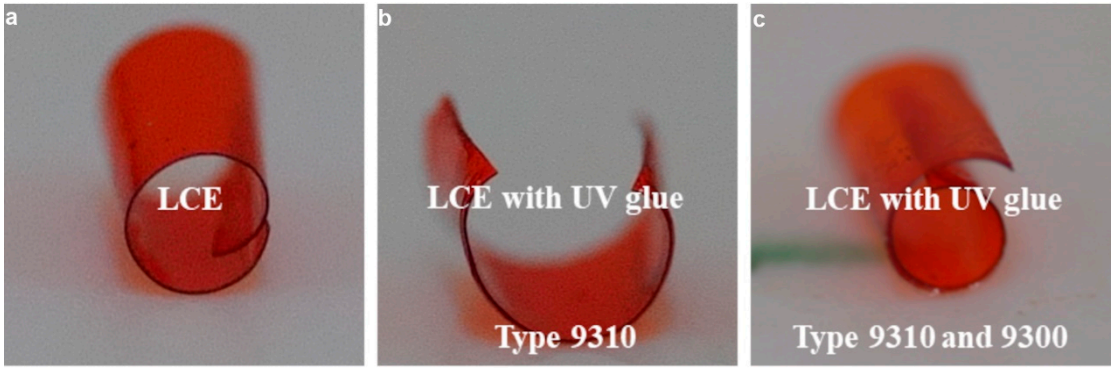

Figure S2. Effect of different UV glues on LCE shape morphing. (**a**) LCE shape morphing without UV glue. (**b**) LCE shape morphing with UV glue Type 9310. (**c**) LCE shape morphing with UV glue mixture of Type 9310 and Type 9300.

3. De-assembly of an LCE film into voxels

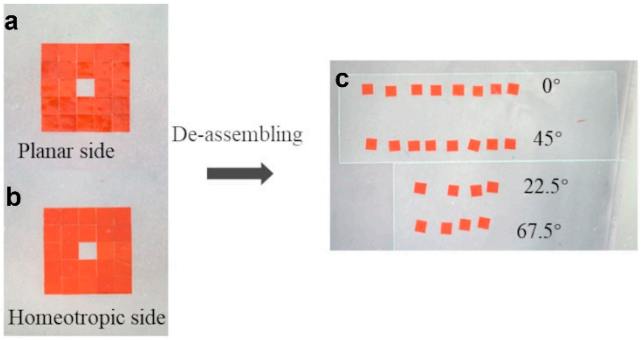

Figure S3. De-assembly of an LCE film into voxels. (**a**) Assembled LCE film viewed from planar side. (**b**) Assembled LCE film viewed from homeotropic side. (**c**) Voxels de-assembled from the LCE film.

4. Thickness of UV glue layer

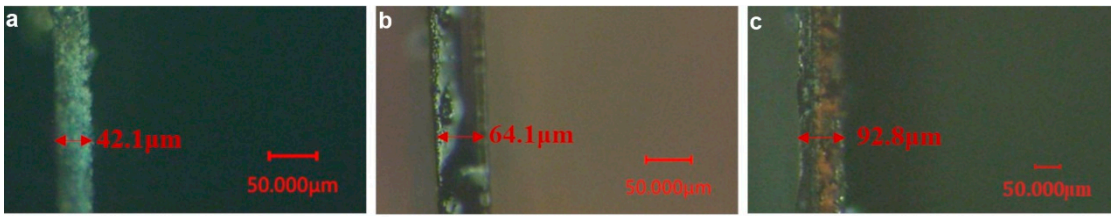

Figure S4. Thickness of UV glue layer. (**a**) Thickness of LCE without UV glue. (**b**) Thickness of LCE film and UV glue after the first assembly. (**c**) Thickness of LCE film and UV glue after the second assembly. The average thickness of UV glue film is around 25 μm.

5. Mechanical properties

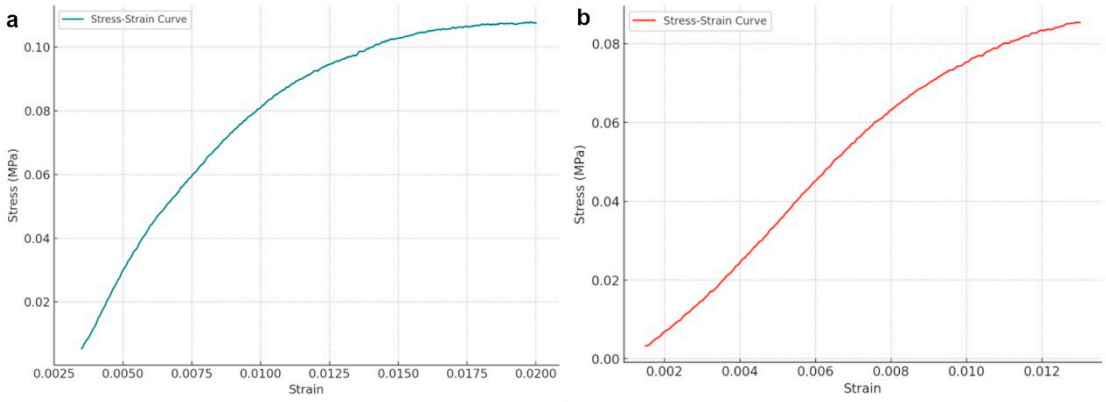

Figure S5. Stress–strain curve for LCE without (a) and with (b) UV glue. We chose the strain range between 0.005 and 0.008 (which corresponds to an approximately linear relation shape between stress and strain) to calculate the Young's modulus. The calculated values were 11.6 Mpa and 9.6 Mpa, respectively.

6. Polarized optical microscopic images

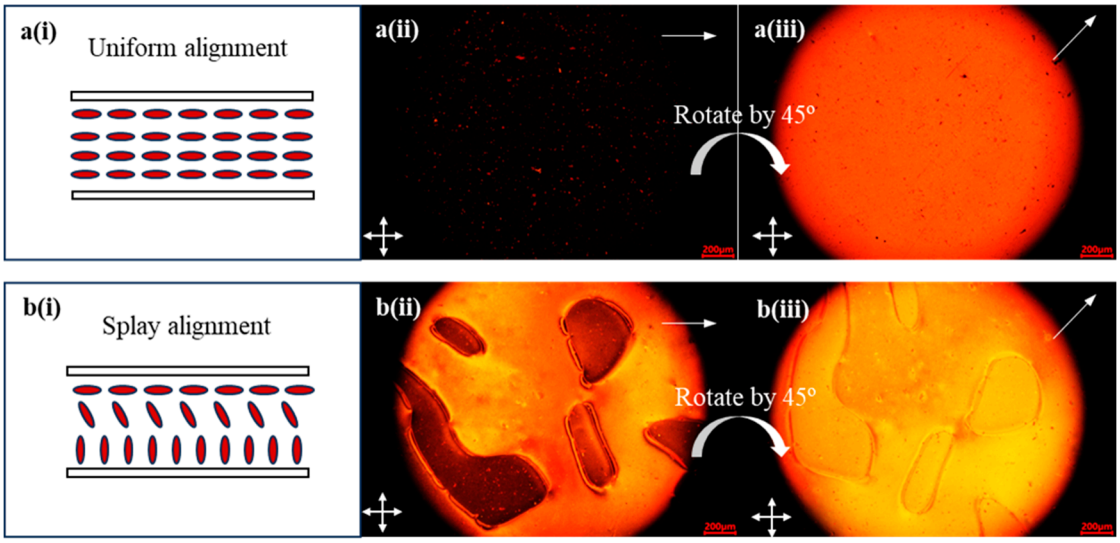

Figure S6. Polarized optical microscopic images of uniform (a) and splay (b) aligned liquid crystal elastomers. Here, a(i) and b(i) are schematics of the corresponding LCE alignment, a(ii) and b(ii) are cross-polarized microscopic images when top surface alignment is along the polarizer axis, and a(iii) and b(iii) are cross-polarized microscopic images when top surface alignment is 45° to the polarizer axis.

7. Durability of LCE samples

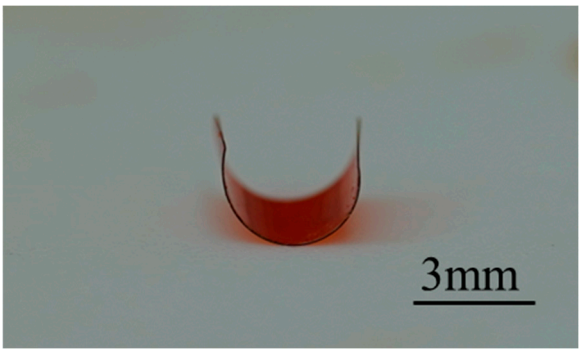

Figure S7. Shape morphing of LCE sample fabricated 3 months prior. The measured bending angle was 194° when heated to 60 ℃, which is close to the value measured in Figure 2 (~190 °).

8. Order of LCE

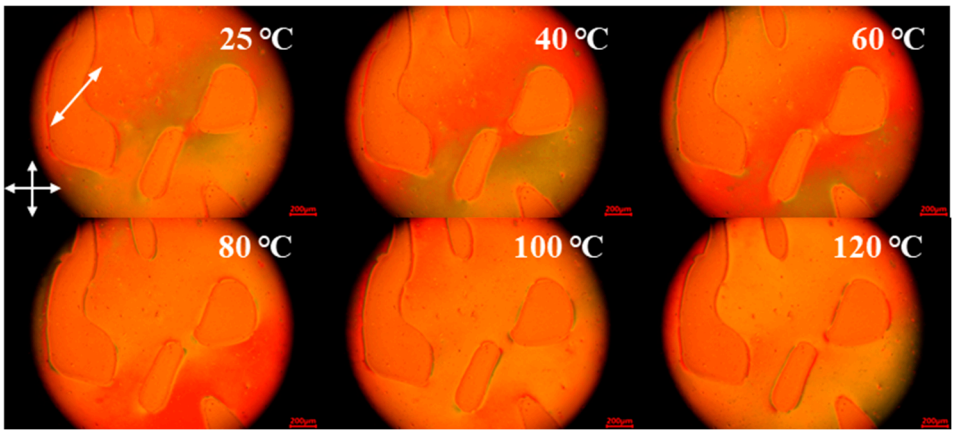

Figure S8. Polarized optical images of LCEs at different temperatures.

9. Reversibility of LCE

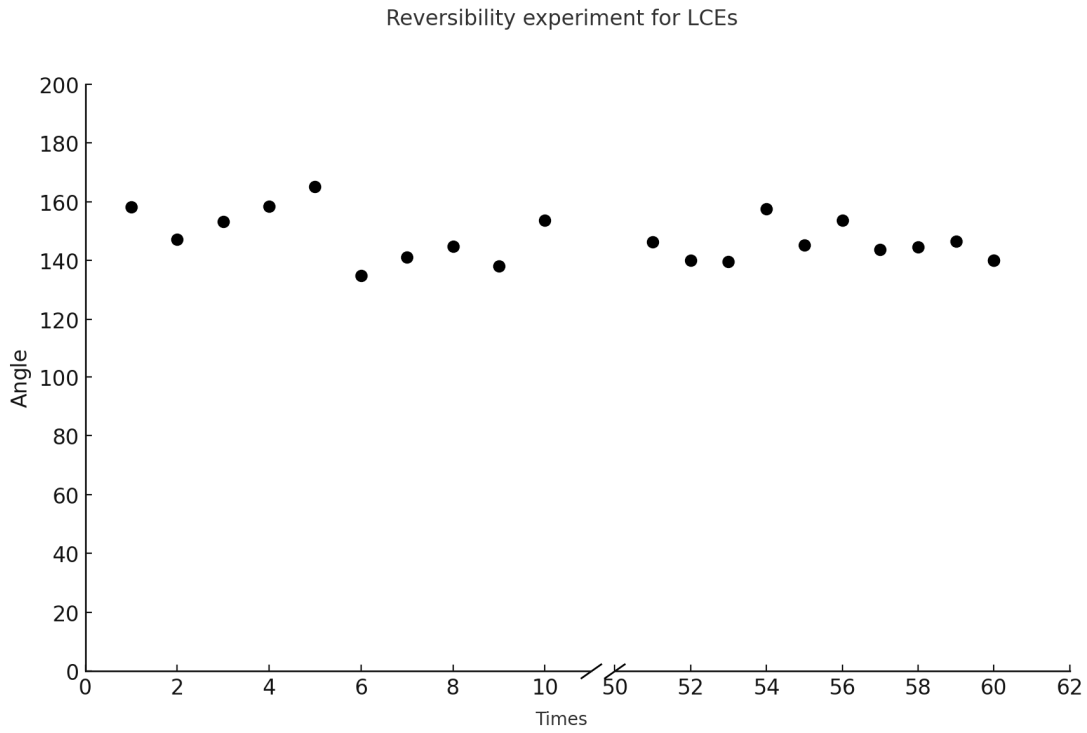

Figure S9. Bending angle of LCE film measured with respect to heating–cooling cycles.

10. Bending curvature with respect to Young's modulus and thickness

Under thermal stimulation, LCEs with complex molecular orientations exhibit nonlinear strains, often requiring complex numerical simulations such as finite element methods for accurate prediction. In this study, to elucidate the relationship between the composite bending deformation of LCEs and UV glue layers and the Young's modulus and thickness of each layer, we constructed an approximate analytical model for the bending strain of composite LCE films. This model is based on the bending equation of planar LCE films. For planar LCE film structures with uniform molecular orientation, the curvature under thermal stimulation—which is related to the strain differential between the two surfaces of the LCE film and its geometric dimensions—can be described using the following relationship:

$$\frac{1}{\rho_1} = \frac{\Delta\varepsilon}{t_1} \quad (1)$$

where ρ_1 represents the radius of curvature, $\Delta\varepsilon$ is the strain differential between the upper and lower surfaces, and t_1 is the thickness of the LCE film. Here, $\Delta\varepsilon$ can be calculated using the equation $(\varphi_2\text{-}\varphi_1)\cdot\Delta T$, where φ_2 and φ_1 are the temperature-responsive coefficients for surfaces with different alignments, and ΔT is the change in temperature. In this study, to explain the relationship between the bending deformation of the bilayer structure of LCE and UV glue, as well as the Young's modulus and thickness of each layer, we consider the LCE film and UV glue layer as a unified two-dimensional planar beam structure. The bending curvature of the bilayer structure is calculated using the equation for the bending of planar beams, as follows:

$$\frac{1}{\rho_{1+2}} = \frac{M}{E_{1+2}\cdot I_{1+2}} \quad (2)$$

where ρ_{1+2} is the radius of curvature for the bilayer composite structure, and M represents the internal bending moment originating from the internal stress caused by the strain differential $\Delta\varepsilon$ in the LCE film layer. E_{1+2} is the equivalent elastic modulus of the bilayer structure, calculated as the weighted average of the elastic moduli E_1, E_2 and the thicknesses t_1, t_2 of the LCE layer and UV glue layer, respectively, given by $\frac{E_1\cdot t_1 + E_2\cdot t_2}{t_1+t_2}$. I_{1+2} represents the equivalent moment of inertia of the section, related to the thicknesses t_1, t_2 of each layer, calculated as $\frac{t_1^3+t_2^3}{12}$. In Equation (1), we can estimate the curvature based on the thickness t_1 of the LCE layer and the strain differential $\Delta\varepsilon$. According to the bending equation $\frac{1}{\rho_1} = \frac{M}{E_1 I_1}$, the internal bending moment M contributed by the

LCE layer can be derived as $M = E_1 \cdot \frac{t_1^3}{12} \cdot \frac{\Delta\varepsilon}{t_1}$. By substituting the values of M, E_{1+2}, and I_{1+2} into Equation (2), we can thus establish the relationship between the curvature of the bilayer structure of LCE and UV glue and the elastic modulus and thickness of each layer, as follows:

$$\frac{1}{\rho_{1+2}} = \frac{E_1 t_1^2 \Delta\varepsilon(t_1+t_2)}{(t_1^3+t_2^3)(E_1 t_1 + E_2 t_2)} \quad (3)$$

Equation (3) reveals that the bending curvature of the bilayer structure exhibits a complex nonlinear relationship with the Young's modulus and thickness of each layer. To visually demonstrate the relationship between curvature changes and the thickness of each layer, we assume that the Young's modulus of each layer remains constant. Under this assumption, we simulate the trend in the normalized radius of curvature ρ_{norm} with varying thicknesses of the UV glue layer, while the thickness of the LCE layer remains fixed. The results are illustrated in Figure S10.

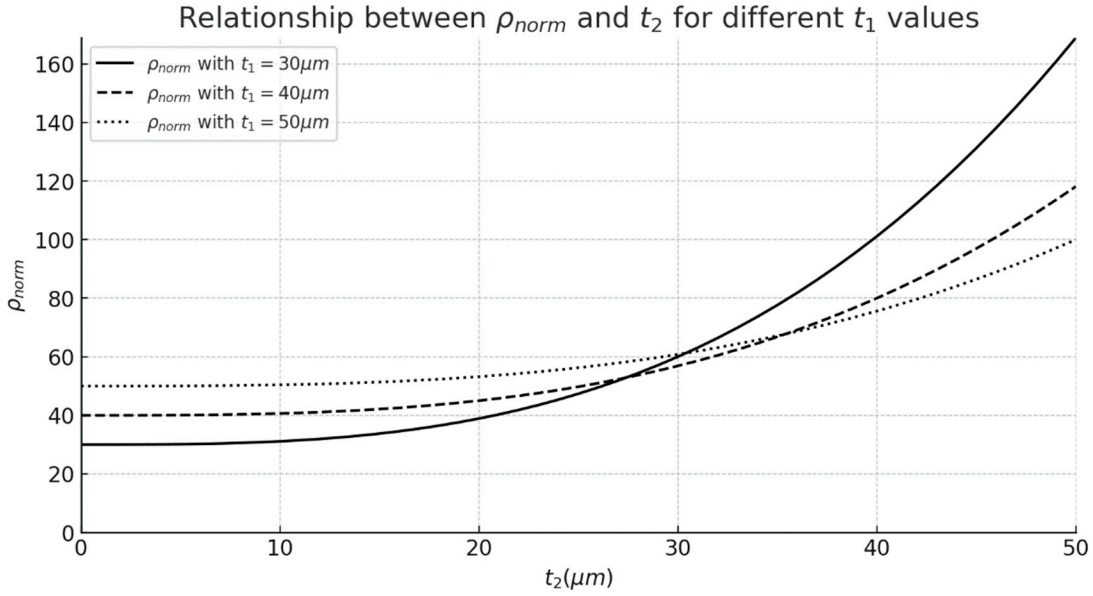

Figure S10. Normalized curvature with respect to thickness of two layers. Assuming the thickness of the LCE layer t_1 is 30, 40, and 50 μm, respectively, and the Young's modulus of each layer E_1, E_2 is constant, the relationship between the normalized radius of curvature ρ_{norm} and the thickness of the UV glue layer t_2 ranges from 0 to 50 μm.